Polymer Brushes that Resist Adsorption of Model Proteins: Design Parameters

A. Halperin

UMR 5819 (CEA-CNRS-UJF), SI3M/DRFMC, CEA-Grenoble, 17 rue des Martyrs, 38054 Grenoble Cedex 9, France

Received September 28, 1998. In Final Form: December 8, 1998

The adsorption of model proteins onto brush-coated surfaces can occur via two modes. Primary adsorption at the surface, where short range attraction is dominant, is important for small proteins and may be repressed by increasing the grafting density. Secondary adsorption, due to van der Waals attraction, occurs at the outer edge of the brush. Large rodlike proteins are likely to adsorb in this fashion. This mode may be repressed by increasing the brush thickness. The thermodynamics and kinetics of adsorption of model proteins are considered within a simple analytical theory distinguishing between the different adsorption mechanisms of small and big proteins.

1. Introduction

Surfaces coated by brushes of terminally grafted, water soluble, chains are highly resistant to protein adsorption in aqueous media. The polymers involved owe their solubility in water to the formation of hydrogen bonds. An important representative of this class is poly(ethylene oxide) (PEO).[1] Such brushes are heavily utilized in order to enhance the biocompatability of materials used in bioengineering applications, pharmaceutics, and biotechnology.[2−4] Self-assembled brushes are of special importance for the protection of soft materials, such as vesicles and proteins, that do not tolerate harsh treatments.[5,6] The efficacy of the brushes is related to two main characteristics: the grafting density σ^{-1} and the brush thickness L_0. In turn, L_0 is determined by the polymerization degree N and by σ^{-1}. In addition, σ^{-1} may depend on the grafting energy of the chain anchor ϵkT and N. The effective choice of σ^{-1} and N varies with the adsorbing protein, its size, concentration, adsorption free energy, and so forth. Accordingly, the optimal characteristics of the brush differ with the protein composition profile of the target environment. The desired lifetime of the device should also be taken into account. Lowering the rate of adsorption may suffice in certain situations while in other cases it is desirable to prevent protein adsorption altogether. Optimizing the design of a protein resistant brush for a given application can be assisted by theoretical arguments relating the many parameters involved. Theoretical aspects of this problem were analyzed numerically by Jeon et al.[7,8] and, more recently, by Szleifer.[9] This article aims to extend their analysis as well as to obtain simple scaling relationships for the various design parameters that control the resistance of polymer brushes to protein adsorption. Following these authors, the analysis is based on two assumptions: First, the polymers are modeled as simple flexible chains. Within this "normal polymer" approximation the distinctive features of water soluble polymers, such as PEO, are ignored. Second, the discussion focuses on model proteins envisioned as dense, rigid objects with nonadsorbing surfaces; that is, the proteins are treated as structureless colloidal particles.

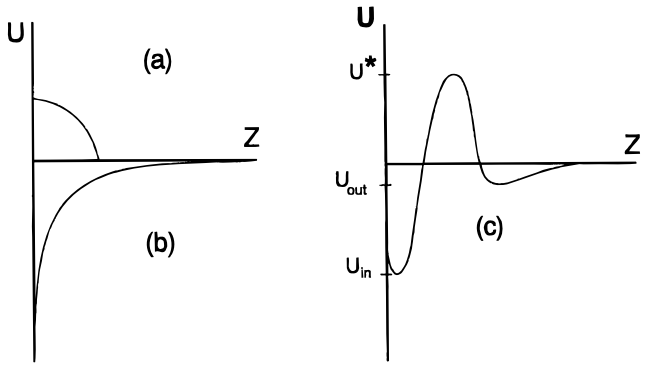

Figure 1. The effective potential U_{eff} experienced by a protein approaching a brush-coated surface (c), which is the result of the superposition of two contributions: (b) the purely attractive interaction potential between the bare surface and the protein U_{bare} and (a) the purely repulsive interaction between the protein and the swollen brush U_{brush}.

A protein that encounters a bare adsorbing surface experiences a purely attractive interaction potential $U_{\text{bare}}(z)$, where z denotes the distance from the surface. The interaction potential is qualitatively modified when the surface is coated by a polymer brush (Figure 1). The overlap of the impenetrable, dense, protein with the brush gives rise to a free energy penalty. This purely repulsive interaction $U_{\text{brush}}(z)$ allows for the work expended in overcoming the osmotic pressure of the brush as the protein approaches the surface. The effective interaction potential between the protein and the brush-coated surface $U_{\text{eff}}(z)$ reflects the superposition of these two contributions, $U_{\text{eff}}(z) = U_{\text{brush}}(z) + U_{\text{bare}}(z)$. Its shape varies with the range and the strength of the two components. In general $U_{\text{eff}}(z)$ may exhibit two minima: a primary minimum adjacent to the surface, of depth U_{in}, and a secondary minimum at the outer edge of the brush, of depth U_{out}. Consequently, it is necessary to allow for two adsorption modes: a

(1) Harris, J. M., Ed. *Poly(ethylene glycol) Chemistry—Biotechnical and Biomedical Applications*; Plenum Press: New York, 1992.
(2) Elbert, D. L.; Hubbell, J. A. *Annu. Rev. Mater. Sci.* **1996**, *26*, 365.
(3) Lee, J. H.; Lee, H. B.; Andrade, J. D. *Prog. Polym. Sci.* **1995**, *20*, 1043.
(4) Malmsten, M. In *Biopolymers at Interfaces*; Malmsten, M., Ed.; Surfactant Science Series; Marcel Dekker: New York, in press.
(5) Lasic, D. D. *Liposomes: From Physics to Applications*; Elsevier: Amsterdam, 1993.
(6) Lasic, D. D.; Papahadjopoulos, D. *Curr. Opin. Solid State Interface Sci.* **1996**, *1*, 392.
(7) Jeon, S. I.; Lee, J. H.; Andarade, J. D.; de Gennes, P. G. *J. Colloid Interface Sci.* **1991**, *142*, 149.
(8) Jeon, S. I.; Andrade, J. D. *J. Colloid Interface Sci.* **1991**, *142*, 159.
(9) Szleifer, I. *Biophys. J.* **1997**, *72*, 595.

10.1021/la981356f CCC: $18.00
Published on Web 03/02/1999

primary adsorption, at the surface, and a secondary adsorption, at the exterior boundary of the brush. These two minima are separated by a maximum whose height is denoted by U^*. Accordingly, the primary adsorption is an activation process while the secondary adsorption is not. Since the barrier crossing in this situation is diffusive, this process may be described by the Kramers rate theory. The shape of U_{eff} as well as the values of U_{in}, U_{out}, and U^* depends on the characteristics of $U_{brush}(z)$ and $U_{bare}(z)$. In certain cases one of the minima, or both, may disappear altogether.

The brush affects the protein adsorption via two routes. First, the strength and the range of $U_{brush}(z)$ are determined by σ^{-1} and by L_0. By varying these parameters, it is possible control the shape of $U_{eff}(z)$, in particular, to tune U_{in}, U_{out}, and U^*. The thermodynamics of the primary and secondary adsorption are controlled, respectively, by U_{in} and U_{out}. The activation barrier U^* is the dominant factor determining the rate of primary adsorption. Second, the viscosity experienced by the protein as it approaches the surface, η, may also increase because of the brush. The analysis of these effects is simplified significantly because of the focus on the resistance to adsorption. Such resistance is attained by tuning the *onset* of adsorption by manipulating the thermodynamics or the kinetics. In the vicinity of the adsorption threshold, the adsorption isotherm and the rate of adsorption depend linearly on the concentration of the protein in solution c. In other words, the fraction of occupied surface sites θ varies as $\theta \approx Kc$, in equilibrium, and the rate of adsorption is $d\theta/dt \approx k_{ads}c$. Furthermore, the density of proteins within the brush at the adsorption threshold is low and the interactions between them may be neglected. Accordingly, it is sufficient to analyze the interaction between a single protein and a brush-coated surface in order to obtain $K(\sigma,N)$ and $k_{ads}(\sigma,N)$. Finally, for the design of resistant brushes it is sufficient to consider the adsorption threshold of the protein species that are most relevant, that is, the proteins that are most susceptible to adsorb or those whose adsorption gives rise to bioincompatability.

For simplicity the discussion is mostly limited to globular, spherical proteins of radius R and to a planar brush consisting of normal, flexible chains. It is assumed that the only interaction between the two is due to the impenetrability of the protein. The extension of this discussion to more complicated geometries is straightforward. This analysis suggests that the adsorption mode depends qualitatively on the R/L_0 ratio. This ratio determines the "mechanism" of primary adsorption and, as a result, the relative importance of the secondary adsorption. Two effects are involved. The R/L_0 ratio affects the qualitative features of both $U_{brush}(z)$ and the hydrodynamic forces that oppose the motion of the protein toward the surface. Large proteins, $R/L_0 \gg 1$ can attain close proximity to the surface only by locally compressing the brush (Figure 2). This "compression" mechanism incurs a heavy free energy penalty first discussed by Jeon et al.[7,8] In addition, this process is opposed by a strong hydrodynamic lubrication force due to the lateral expulsion of the solvent residing between the protein and the surface.[10] As a result, large proteins are prone to secondary adsorption, at the outer boundary of the brush, where van der Waals attraction to the surface may be important. As we shall see, secondary adsorption is expected to be of particular importance in the case of large rodlike proteins. This adsorption mode may be repressed by increasing the brush thickness, L_0. On the other hand, only weak perturbation of the brush is expected when small proteins, $R/L_0 \ll 1$, approach the surface (Figure 3). This scenario

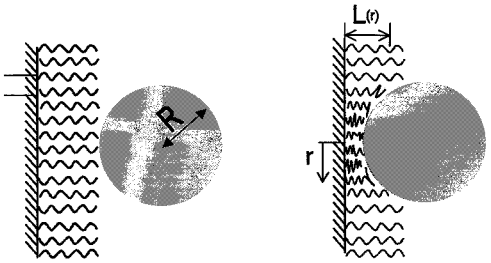

Figure 2. Large proteins can approach the surface only by compressing the brush. The free energy penalty associated with the compression mechanism favors secondary adsorption at the outer edge of the brush.

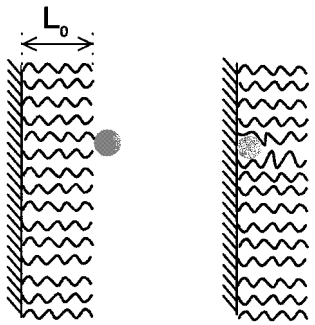

Figure 3. Small proteins, $R < L_0$, can penetrate the brush with little effect on its overall concentration profile. This insertion mechanism favors primary adsorption at the surface.

was first considered, implicitly, by Szleifer.[9] The free energy penalty associated with this "insertion" mechanism is much smaller in comparison to that characterizing the compression case. In addition, the hydrodynamic force that opposes the insertion process is the Stokes' drag force, which is much weaker than the lubrication force encountered in the compressive mechanism. Consequently, small proteins preferentially penetrate the brush and undergo primary adsorption at the surface, where strong short range attractive interactions are important. This adsorption mode is most sensitive to σ and may be repressed by increasing the grafting density.

General considerations that apply to both limits are presented in section 2. These include a discussion of the interactions giving rise to $U_{bare}(z)$, as well as of some of the length and energy scales. The relationships between U_{in}, U_{out}, and the adsorption isotherm are briefly described. The secondary adsorption of big proteins is discussed as well as the design parameters for its repression. In addition, the Kramers rate theory that can describe the primary adsorption of small proteins is reviewed. The structure of planar brushes in good solvents is briefly summarized in section 3. Two approximate views are presented. One is the Alexander model, in which the brush is described by a steplike concentration profile. The second is the Pincus approximation that leads to a parabolic concentration profile. This discussion serves to introduce the important length scales as well as the necessary background for calculating U_{brush}. The thermodynamics and the kinetics of the insertion mechanism, $R/L_0 \ll 1$, are discussed in section 4. Section 5 is devoted to the thermodynamics of the compression mechanism, $R/L_0 \gg 1$, with some limited discussion of the kinetics. In certain situations σ and L_0 are not independent variables, as is assumed in sections 3−5. The resulting modifications are discussed in section 6. The role of the end groups as well as the limitations of a description ignoring the special features of water soluble chains is discussed in sections 7 and 8.

2. Thermodynamics, Kinetics, and the Kramers Rate Theory

Understanding of the adsorption of proteins onto brush-coated surfaces requires knowledge of the interaction potential $U_{eff}(z)$. With some important caveats, to be discussed later, the brush contribution to $U_{eff}(z)$, $U_{brush}(z)$, is well understood. The situation with regard to the interaction potential between the bare adsorbing surface and the protein $U_{bare}(z)$ is less favorable. Electrostatic and van der Waals energies contribute $U_{bare}(z)$. $U_{bare}(z)$ also reflects solvation effects, hydrogen bonding, and other short range interactions.[11] The reported effect of Ca^{2+} ions[2] suggests that ion correlations may be important. The relative weights of the various terms vary with the protein and the surface. The detailed functional form of $U_{bare}(z)$ is typically unknown. It is thus difficult to obtain the exact functional form of $U_{eff}(z)$. Nevertheless it is possible to proceed if two conditions are satisfied: (i) The range of the strongly attractive part of $U_{bare}(z)$ is very short in relation to the range of $U_{brush}(z)$. (ii) The long range component of $U_{bare}(z)$ is negligible in comparison to $U_{brush}(z)$ throughout the brush. It may however exceed the thermal energy kT at the outer boundary of the brush, around $z \approx L_0$. This last component certainly involves van der Waals attraction though hydrophobic and screened electrostatic interactions as well as solvation effects may contribute. It is not clear that these conditions are always satisfied. The first requirement is fulfilled in the limit of thick brushes. The second is met in solutions of high ionic strength because of the resulting screening of electrostatic interactions. In the following we assume that these two requirements are satisfied for the situations of interest involving brushes that retard protein adsorption in biological fluids of high ionic strength.

Having made this assumption, the analysis of this scenario depends on a single characteristic of $U_{bare}(z)$, the depth of the minimum at the surface U_{ads}. This parameter is specified by the linear regime of the adsorption isotherm. In this range the adsorbed proteins form a dilute two-dimensional solution at the surface; that is, the fraction of occupied adsorption sites is $\theta \ll 1$. The chemical potential of the adsorbed proteins is then $\mu_{ads} \approx U_{ads} + kT \ln \theta$, where U_{ads} is measured with respect to a free isolated protein in a dilute solution. In this convention, the chemical potential of the free proteins in the solution is $\mu_{free} \approx kT \ln c$. Accordingly, $\theta \approx K_{bare}c$, where the equilibrium constant is $K_{bare} \approx \exp(-U_{ads}/kT)$. Note, however, that the linear part of the isotherm is typically very steep, and it is thus difficult to accurately specify U_{ads}. Within this approximation the adsorption isotherm of the brush-coated surface may reflect either one or two contributions. Primary adsorption at the surface gives rise to $\theta_{in} \approx K_{in}c$, where $K_{in} \approx \exp(-U_{in}/kT)$ and

$$U_{in} \approx U_{ads} + U_{brush}(0) \tag{1}$$

In addition, a secondary adsorption at the outer edge of the brush is possible if $U_{bare}(L_0) > kT$. The secondary adsorption is described by $\theta_{out} \approx K_{out}c$, where $K_{out} \approx \exp(-U_{out}/kT)$. When both adsorption modes are operative, at the adsorption threshold, we may assume that θ_{in} and θ_{out} are independent. In this situation the total amount of adsorbed protein Γ is roughly proportional to $\theta_{in} + \theta_{out}$; that is, $\Gamma \sim (K_{in} + K_{out})c$. To analyze the primary adsorption, it is necessary to specify $U_{brush}(z)$. This, in turn, depends on the size of the globular protein R. As we shall discuss in the following sections, different behavior is expected for $(R/L_0) \gg 1$ and for $(R/L_0) \ll 1$. The secondary adsorption behavior is conceptually simpler. The condition $U_{out}/kT \gtrsim 1$ is sufficient for the occurrence of secondary protein adsorption at the edge of the brush, irrespective of the value of R/L_0. In this case the long range interaction between the surface and the protein at the edge of the brush is strong enough but the protein is expelled from the brush itself because of the osmotic price of achieving closer proximity to the surface. This consideration can lead to explicit design parameters, provided the functional form of the long range tail of U_{bare} is known. Of the possible interactions invoked, only the van der Waals attraction is fully understood. In the case of spherical, globular proteins, the van der Waals interaction is typically too weak. The attraction energy between a sphere and a planar "half-space" is $U_{vdW} \approx -AR/6L$, where L is the distance of closest proximity between the two and A is the Hamaker constant.[12] The $U_{out}/kT \approx 1$ criterion is not satisfied for $L_0 \approx 3$ nm, even for very big proteins, $R \approx 9$ nm. On the other hand, $U_{out}/kT > 1$ can be obtained for rodlike proteins when the major axis is parallel to the surface. The van der Waals attraction between a rod of radius R and length H may be approximated as

$$U_{vdW} \approx -\frac{AR^{1/2}H}{12\sqrt{2}L_0^{3/2}} \tag{2}$$

For example, if fibrinogen is modeled as a rod of $H \approx 55$ nm and $R \approx 10$ nm, the corresponding U_{vdW} is comparable to kT for $L_0 \approx 3$ nm. This discussion suggests that big rodlike proteins may preferentially undergo secondary adsorption. Furthermore, the repression of the secondary adsorption of rodlike protein may be accomplished by increasing L_0 above

$$L_{rod} \approx \left(\frac{A}{12\sqrt{2}kT}\right)^{2/3} R^{1/3}H^{2/3} \tag{3}$$

This argument may be used to explain the dependence of the adsorption isotherm on N, in particular, the occurrence of saturation, that is, a maximal N_{max} such that for $N \geq N_{max}$ the adsorbed amount is independent of N, that is, $\Gamma \sim N^0$. Note that the control of primary adsorption and of secondary adsorption involves different design parameters. While L_0 controls the secondary adsorption, the primary adsorption is controlled, as we shall discuss, by σ.

Primary adsorption onto the brush-coated surface is an activation process. To reach the surface, the protein must first overcome a free energy barrier. This process involves a diffusive motion of a classical particle through a fluid medium. It is thus described by the Kramers rate theory.[13−15] This generalization of the transition-state theory allows for the effect of random forces, generated by the solvent, on the rate of the reaction. The high viscosity limit of this theory applies to the primary adsorption scenario. This yields the following expression for the adsorption rate constant, as defined by $d\theta/dt = k_{ads}c$,

$$k_{ads} \approx \exp(-U^*/kT)D/\alpha L_0 \tag{4}$$

(10) Fredrickson, G. H.; Pincus, P. *Langmuir* **1991**, *7*, 786.
(11) Haynes, C. A.; Norde, W. *Colloids Surf., B* **1994**, *2*, 517.
(12) Israelachvili, J. N. *Intramolecular and Surfaces Forces*, 2nd ed.; Academic Press: London, 1991.
(13) Kramers, H. A. *Physica* **1940**, *7*, 284.
(14) Chandrasekhar, S. *Rev Mod. Phys.* **1943**, *15*, 1.
(15) Halperin, A. *Europhys. Lett.* **1989**, *8*, 351.

Here D is the appropriate diffusion coefficient and α is the width of the barrier kT below U^*. A simple derivation of this expression is described in Appendix I. Essentially, $\exp(-U^*/kT)$ of the proteins adjacent to the brush possesses the free energy that allows them to cross the barrier. In the high-viscosity limit these "activated" particles diffuse across the barrier. This process is assumed to be slow enough so as to allow the equilibration of the protein population. The characteristic time of the barrier crossing $\tau_{barrier}$ is specified by the Einstein diffusion relation $\tau_{barrier}D \approx \alpha^2$. D/α is the effective velocity of the diffusive *current* across the barrier. In marked contrast to the case of the transition-state theory, the average velocity of the particles crossing the barrier is zero. $v_{diff} \approx \exp(-U^*/kT)D/\alpha$ is the velocity of the steady-state diffusive flux across the barrier. The characteristic time for traversing a barrier of width L_0 is thus L_0/v_{diff} and the corresponding unimolecular rate constant is $k_{ads} \sim v_{diff}/L_0$. Notice that within the Kramers rate theory k_{ads} depends only on two coarse-grained characteristics of $U_{eff}(z)$, namely α and U^*. A precise functional form of $U_{eff}(z)$ is not required. The detailed implementation of the Kramers rate theory to the primary adsorption case will be described in section 4.

The rate of primary adsorption is determined mostly by U^*. The thermodynamic equilibrium described by the adsorption isotherm is controlled by $U_{in} \approx U_{ads} + U_{brush}(0)$. Primary adsorption may be suppressed thermodynamically by increasing U_{in} or kinetically by increasing U^*. Accordingly, even when $U_{in}/kT \ll 0$, the adsorption may be negligible for prolonged periods if $U^*/kT \gg 1$.

3. Polymer Brushes: A Reminder

The length scales, free energy, and osmotic pressure of brushes are the key ingredients of our analysis. While the theory of brush structure has been extensively reviewed,[16,17] it is nevertheless helpful to recall its key features. The Alexander model is a good starting point for such a discussion.[18] It describes the underlying physics, yields most of the necessary information, and provides the required background for more elaborate descriptions. The model considers a flat brush of flexible chains comprising each N monomers of size a. The area per grafted headgroup σ is small enough to ensure chain overlap. In a good solvent $\sigma \leq R_F^2$, where $R_F \approx N^{3/5}a$ is the Flory radius of the free chain, while in a θ solvent $\sigma \leq R_0^2$, where $R_0 \approx N^{1/2}a$. When σ is larger, in the "mushroom regime", the chains do not crowd each other, thus retaining, essentially, their free bulk configurations. In the following we focus, for brevity, on the case of brushes immersed in athermal good solvents; that is, the Flory χ parameter is zero and, equivalently, the second virial coefficient is $v \approx a^3$. The chain crowding increases the number of repulsive monomer−monomer contacts. Consequently, the brush swells along the normal to the surface in order to lower the interaction free energy at the price of a higher stretching free energy penalty. Within the Alexander model, the brush is described by a steplike concentration profile. In a brush of thickness L the monomer volume fraction is $\phi \approx Na^3/L\sigma =$ constant, where $L\sigma$ is the volume per chain. All chains are assumed to be uniformly stretched with their free ends localized at L. The free energy per chain reflects two contributions, $F_{chain} = F_{int} + F_{el}$, allowing respectively for monomer−monomer interactions and the elasticity of the chain. The elastic free energy of a uniformly stretched chain is $F_{el}/kT \approx L^2/R_0^2$. It reflects the elastic work $f_{el}dL$ performed by the elastic force $f_{el}/kT \approx L/R_0^2$ as the chain stretches from R_0 to L. F_{int} allows for the corresponding work done by the osmotic pressure of the brush π, $-\pi\sigma dL$, leading to $F_{int} = \pi\sigma L$. The equilibrium state of the brush is specified by $\partial F_{chain}/\partial L = 0$. In the equilibrium state the two terms are comparable,

$$\pi\sigma/kT \approx L/R_0^2 \tag{5}$$

that is, the osmotic force is balanced by the elastic one. The precise form of π and R_0 depends on the adopted approximation. Within the Flory version of the Alexander model the brush consists of ideal chains that interpenetrate freely and exhibit no correlations. In this case $\pi a^3/kT \approx \phi^2$ and $R_0 \approx N^{1/2}a$. Both F_{int} and F_{el} are overestimated within this approximation. These two errors cancel when $\partial F_{chain}/\partial L = 0$ is used to obtain the equilibrium thickness, thus leading to

$$L_0/a \approx N(a^2/\sigma)^{1/3} \tag{6}$$

and to the equilibrium monomer volume fraction

$$\phi_0 \approx (a^2/\sigma)^{2/3} \tag{7}$$

The corresponding osmotic pressure $\pi_0 a^3/kT \approx \phi_0^2 \approx (a^2/\sigma)^{4/3}$ and free energy $F_0/kT \approx N(a^2/\sigma)^{2/3}$ are both overestimated. The Flory approximation, because of its simplicity, will nevertheless serve us later in introducing a more realistic description of the brush concentration profile. The correlations within the system are taken into account within the blob picture. In this scheme the brush is envisioned as a close-packed array of blobs of size $\xi \approx \phi^{-3/4}a$ comprising each a self-avoiding chain segment of g monomers such that $\xi \approx g^{3/5}a$ and $g \approx \phi^{-5/4}$. Each chain is viewed as a string of N/g blobs. Since the correlations are screened over distances larger than the correlation length ξ, the unperturbed chain span is $R_0 \approx (N/g)^{3/5}\xi \approx N^{1/2}\phi^{-1/8}a$. Each blob is assigned an energy of kT. The osmotic pressure is thus $\pi \approx kT/\xi^3 \approx \phi^{9/4}$. In equilibrium, when $\phi_0 \approx (a^2/\sigma)^{2/3}$, the average blob size is

$$\xi_0 \approx \sigma^{1/2} \tag{8}$$

the osmotic pressure is

$$\pi_0 a^3/kT \approx \phi_0^{9/4} \approx (a^2/\sigma)^{3/2} \tag{9}$$

and the free energy per chain $F_0 \approx \pi_0\sigma L_0$ is

$$F_0/kT \approx N(a^2/\sigma)^{5/6} \tag{10}$$

The free energy per chain upon compression to $L < L_0$ may be expressed as[16,17]

$$\frac{F}{kT} \approx \frac{F_0}{kT}\left[\left(\frac{L_0}{L}\right)^{5/4} + \left(\frac{L}{L_0}\right)^{7/4}\right] \tag{11}$$

Note that within this view the equilibrium state corresponds to a fully stretched string of blobs; that is, $L_o \approx (N/g)\xi_0$. The correlation length ξ_0 introduced in this picture will play an important role in the subsequent discussion, since it affects both the thermodynamics and the dynamics of protein adsorption.

The Alexander model constrains the chain ends to a single altitude. The free energy of the brush is lowered when this constraint is relaxed. A simple approximation

(16) Milner, S. T. *Science* **1991**, *251*, 905.
(17) Halperin, A.; Tirrell, M.; Lodge, T. *Adv. Polym. Sci.* **1992**, *100*, 31.
(18) Alexander, S. *J. Phys. (Paris)* **1977**, *38*, 977.

describing this scenario was recently introduced by Pincus.[19] This approximation occupies the middle ground between the Alexander model and the full self-consistent field theory of the brush. Within this picture the chain ends are distributed throughout the brush and the mean free energy per unit area is $\gamma = \int_0^L F_{\text{brush}}(z)\,dz$, where $F_{\text{chain}} = \sigma\gamma$ and the free energy density is

$$\frac{F_{\text{brush}}}{kT} \approx a^{-3}\left[\phi^2(z) + \frac{z^2}{Na^2}\Psi(z) - \lambda\phi(z)\right] \qquad (12)$$

The first term, allowing for monomer−monomer interaction, is π/kT. This term is appropriate when the brush is semidilute. The handling of the elastic free energy penalty is the core of the Pincus approximation. A chain having its end point at altitude z is assumed to be a uniformly extended Gaussian spring with a free energy penalty $F_{\text{el}}/kT \approx z^2/Na^2$. Notice that within the full SCF theory the chain stretching may vary along the chain. The end points are assumed to be distributed throughout the layer with a density $\Psi(z)$. The key assumption is that the local fraction of chain ends $\Psi(z)$ is proportional to the local concentration and to the fraction of chain ends within the chain itself $1/N$. In other words

$$\Psi(z) \approx \phi(z)/N \qquad (13)$$

Note that in this approximation the end point distribution is *assumed* rather than derived, as is the case in the SCF theory. Furthermore, $\Psi(z)$ is wrong for small altitudes. Nevertheless, this approximation yields the correct concentration profile because $F_{\text{el}} \sim z^2$ and the large z contribution, where this assumption is reasonable, dominates. Finally, λ is a Lagrange parameter fixing the number of monomers per chain N. The equilibrium state of the brush is specified by $\delta\gamma/\delta\phi = \partial F_{\text{brush}}/\partial\phi = 0$, leading to a parabolic concentration profile $\phi(z) \approx \lambda - z^2/N^2a^2$. λ is determined by the constraint $Na^3 = \sigma\int_0^L \phi\,dz$ together with the requirement that $\phi(L_0) = 0$. For an unperturbed brush at equilibrium, this yields $L_0 \approx N(a^2/\sigma)^{1/3}a$ and $\lambda_0 \approx (a^2/\sigma)^{2/3}$, leading to

$$\phi_0(z) \approx \left(\frac{a^2}{\sigma}\right)^{2/3}\left(1 - \frac{z^2}{{L_0}^2}\right) \qquad (14)$$

The Pincus approximation recovers the parabolic profile as obtained analytically by SCF theories considering the strong stretching limit, that is, when the chain trajectories fluctuate weakly around a single strongly stretched configuration. The agreement with this picture for a given σ increases with N. For finite N the concentration profile is not strictly parabolic. A maximum is found near the surface while at the surface itself the concentration is zero. The distal part of the brush extends beyond the limit suggested by the parabolic profile. Both deviations were observed in simulations, as well as numerical self-consistent field studies. These effects are negligible for our analysis, since the uncertainties associated with U_{bare} are far larger.

4. Invasive Mechanism

When the protein is small enough, it may penetrate the layer with little effect on the concentration profile (Figure 3). Roughly speaking such is the case for spherical proteins with $R \ll L_0$. The protein will nevertheless experience the effect of the brush if $R > \xi_0$. This section is thus devoted to the "invasive mechanism" occurring when $\xi_o < R \ll L_0$. The first issue, and the simplest, concerns the thermodynamics of primary adsorption. The adsorption isotherm is specified by the equilibrium constant $K_{\text{in}} \approx \exp(-U_{\text{in}}/kT)$, where $U_{\text{in}} \approx U_{\text{ads}} + U_{\text{brush}}(0)$. In the invasive mode U_{brush} is due to the impenetrability of the protein. Upon insertion into the brush, the volume occupied by the protein $\sim R^3$ becomes inaccessible to the monomers. This gives rise to an osmotic penalty, $U_{\text{brush}}(z) \approx \pi(z)R^3$. The Alexander model is sufficient to identify the functional form of U_{in}. In this case $\pi(z) \approx \pi_0 \approx kT/{\xi_0}^3$, leading to $U_{\text{brush}} \approx kT(R/\sigma^{1/2})^3$. Accordingly

$$U_{\text{in}} \approx U_{\text{ads}} + kT(R/\sigma^{1/2})^3 \qquad (15)$$

The adsorption is effectively repressed when $U_{\text{in}}/kT \gtrsim 1$, thus specifying a crossover grafting density of σ_{co}^{-1} given by

$$\sigma_{\text{co}} \approx R^2(kT/|U_{\text{ads}}|)^{2/3} \qquad (16)$$

When $|U_{\text{ads}}|/kT > 1$, this condition requires that $R \approx \xi_0(|U_{\text{ads}}|/kT)^{1/3} > \xi_0 \approx \sigma^{1/2}$; that is, the osmotic penalty is significant when the protein is much bigger than the blob size. Note that when σ is independent of N, the isotherm depends only on the grafting density.

The adsorption rate constant k_{ads} requires a more detailed analysis. Within the Kramers model k_{ads} depends on three characteristics of U_{brush}, namely U^*, α, and L_0. In addition it depends on the diffusion coefficient of the protein within the brush D_{brush}. In turn, D_{brush} depends on the viscosity experienced by the protein as it moves in the brush. In a semidilute solution of entangled chains, this viscosity is expected to vary with R. When R is small compared to the "mesh size" ξ_0, the protein experiences the viscosity of the solvent η_s. On the other hand, proteins that are bigger than L_0 are expected to experience the macroscopic viscosity of the polymer solution.[20] The viscosity of the brush is similar to that of a semidilute solution of entangled chains. The dense grafting gives rise to an elastic modulus, $kT/{\xi_0}^3$. In addition, the chains in the brush are strongly stretched and their longest relaxation time is the reptation time $\tau_{\text{rep}} \approx \eta_s {L_0}^3/kT$, even in the absence of entanglements.[21] Accordingly (Appendix II)

$$\eta(R) \approx \eta_s(R/\xi)^3 \qquad \xi < R < L_0 \qquad (17)$$

With this in mind, we are in a position to obtain k_{ads} within the Alexander model. Because of the assumption of a steplike concentration profile $\alpha \approx L_0$, $U_{\text{brush}}(z) \approx \pi_0 R^3 \approx kT(R/\sigma^{1/2})^3 \approx U^*$ and

$$D_{\text{brush}} \approx \frac{kT}{\eta R} \approx \frac{kT}{\eta_s R}\left(\frac{\sigma^{1/2}}{R}\right)^3 \qquad \xi < R \ll L_0 \qquad (18)$$

leading to

$$k_{\text{ads}} \approx \exp[-(R/\sigma^{1/2})^3]\,\frac{kT}{\eta_s R {L_0}^2}\left(\frac{\sigma^{1/2}}{R}\right)^3 \qquad \xi < R \ll L_0 \qquad (19)$$

k_{ads} decreases as $R/\sigma^{1/2}$ increases, both because of the increase in U^* and the decrease of D_{brush}. However, the exponential effect of U^* is dominant. In addition, k_{ads}

(19) Pincus, P. *Macromolecules* **1991**, *24*, 2912.

(20) de Gennes, P. G. *Scaling Concepts in Polymer Physics*; Cornell University Press, Ithaca, NY, 1979.

(21) Halperin, A.; Alexander, S. *Europhys. Lett.* **1988**, *6*, 439.

decreases as $L_0^{-2} \sim N^{-2}$. This effect as well is secondary in comparison to $\exp(-U^*/kT)$. The ratio $R/\sigma^{1/2}$ is thus the leading control parameter for the control of k_{ads}. Note that small proteins with $R \leq \sigma^{1/2}$ are no longer affected by the brush.

The Alexander model clearly overestimates α. A parabolic profile will undoubtedly yield $\alpha < L_0$. A rough estimate of α may be obtained if we consider a brush described by

$$\phi_0(z) \approx \phi_0\left(1 - \frac{z^2}{{L_0}^2}\right) \tag{20}$$

where $\phi_0 \approx (a^2/\sigma)^{2/3}$. The problem is that this functional form does not describe a brush in an athermal good solvent. In this case the z/L_0 dependence is expected to have a slightly different exponent. In view of the roughness of our description, we will ignore this point and estimate $\pi_0(z)a^3/kT \approx {\phi_0}^{9/4}(1 - z^2/{L_0}^2)^{9/4}$. As before, $U_{brush}(z) \approx \pi_0(z)R^3$; however, in this case U_{brush} varies with z.

$$\frac{U_{brush}(z)}{kT} \approx \left(\frac{R}{\sigma^{1/2}}\right)^3\left[1 - \left(\frac{z}{L_0}\right)^2\right]^{9/4} \tag{21}$$

α is specified by $U_{brush}(0) - U_{brush}(\alpha) \approx kT$. For the case of $\sigma^{1/2} \ll R \ll L_0$ this leads to

$$\alpha \approx \left(\frac{\sigma^{1/2}}{R}\right)^{3/2} L_0 \tag{22}$$

On the other hand $\alpha \approx L_0$ when $R \lesssim \sigma^{1/2}$.

5. Compressive Mechanism

The picture described in the previous section is qualitatively modified for big proteins, $R \gg L_0$. Three effects are involved. First, large proteins can approach the surface only by compressing the layer (Figure 2). This gives rise to a much steeper $U_{brush}(z)$. Furthermore, in this case the protein may be unable to attain direct contact with the surface. When $\sigma = Na^2$, a strongly compressed brush forms a monolayer of thickness a. Dense, continuous layers of width $L_{min}/a \approx N(a^2/\sigma)$ form when $\sigma < Na^2$. In turn, the formation of such dense polymer layers modifies the short range interactions between the protein and the surface, since it sets a limit to the closest approach and prevents contact interactions. Finally, the hydrodynamics involved are fundamentally different. The friction coefficient of small proteins is due to the drag force, as given by the Stokes law, thus leading to $\eta \approx 6\pi\eta_s R$. Lubrication forces should dominate the approach of big proteins. Even in the absence of a brush this is an important effect, since the associated hydrodynamic force is

$$f = -6\pi\eta_s R^2\frac{\dot{L}}{L} \tag{23}$$

where $\dot{L}$ is the velocity along the normal to the surface. In the case of a surface coated by a brush, the lubrication force is stronger[10]

$$f = -\frac{4}{3}\pi\eta_s R^2\left(\frac{L}{\xi(L)}\right)^2\frac{\dot{L}}{L} \tag{24}$$

All three factors enhance the effectiveness of the brush in preventing protein adsorption. Unfortunately, these factors also prevent the full implementation of the analysis presented in section 4. One difficulty is that a different free energy is required in order to describe the full compression range. Ternary and higher order interactions cannot be neglected for dense layers. Second, the Kramers rate theory is no longer applicable because the adsorption in the compressive mode involves displacements that are much smaller than R. Accordingly, a description assuming diffusive motion on such length scales is not justified. A semiqualitative study of the compressive adsorption mode is however possible assuming that U_{eff} reflects a competition between van der Waals attraction and the brush term, that is, that the dominant contribution to the long-range component of U_{bare} is due to van der Waals interaction.

U_{brush} of big proteins is sensitive to the shape of the protein. To obtain U_{brush} in this limit, it is necessary to utilize the Derjaguin approximation.[10,12] The geometry of the system involving a spherical protein approaching a flat brush is explained in Figure 2. The distance of closest approach between the surfaces is denoted by L. The distance between the two surfaces, as a function of the in-plane distance from the point of closest approach r, is

$$L(r) \approx L + \frac{r^2}{2R} \tag{25}$$

The contact area extends from $r = 0$ to $r \approx r_u$, defined by $L(R_u) \approx L_0$ or ${r_u}^2 \approx 2R(L_0 - h)$. The Derjaguin approximation for U_{brush} is

$$U_{brush} = \int_0^{r_u}(F_{chain}/\sigma)r\,\mathrm{d}r \tag{26}$$

For the description of the compressive mechanism, the Alexander model is sufficient. The full SCF calculation differs only in a weak high-order correction term. Using the blob version of the Alexander model, as given by eq 11, and omitting numerical prefactors and constant terms, we obtain

$$U_{brush} \approx \frac{F_0 R L_0}{\sigma}\left[\left(\frac{L_0}{L}\right)^{1/4} - \left(\frac{L}{L_0}\right)^{11/4}\right] \tag{27}$$

For specificity, the long range component of U_{bare} is identified with the van der Waals interaction between a sphere and a surface

$$U_{bare} \approx -\frac{AR}{L} \tag{28}$$

where A is the Hamaker constant. The corresponding U_{eff} is

$$U_{eff} \approx \frac{F_0 R L_0}{\sigma}(u^{-1/4} - u^{11/4} - \kappa u^{-1}) \tag{29}$$

where $u = L/L_0 \leq 1$. $\kappa \approx A\sigma/F_0{L_0}^2$ is the ratio of the van der Waals attraction at L_0, AR/L_0, and the free energy of the unperturbed brush "patch" that interacts with the protein, F_0RL_0/σ. κ measures the relative importance of the brush penalty. When κ is large, the van der Waals attraction dominates and U_{eff} is purely attractive. A potential barrier develops as κ decreases. Quantitatively, $\mathrm{d}U_{eff}/\mathrm{d}u = 0$ leads to $u^{3/4} + u^{15/4} \approx \kappa$, which has a physical solution, $u \leq 1$, for $\kappa \lesssim 0.7$. For smaller κ, the position of the maximum is roughly

$$u^* \approx \kappa^{4/3} \tag{30}$$

and its height is approximately

$$U^* \approx \frac{F_0 R L_0}{\sigma} \kappa^{-1/3} \sim \frac{{L_0}^2 R}{\sigma^{3/2}} \sim \frac{N^3 R}{\sigma^3} \tag{31}$$

Notice that u^* decreases as κ increases, thus indicating that the maximum approaches the surface. The barrier height increases concomitantly. As noted before, closer approach densifies the layer and the free energy used above is no longer applicable. Eventually closer approach to the surface is prevented because of the formation of a dense polymer layer separating the protein from the surface. As opposed to the insertion mechanism, where U^* is independent of N, in the compression mode, $U^* \sim N^3$. Since $k_{ads} \sim \exp(-U^*/kT)$, the kinetics of the compressive mode are very slow. It thus seems likely that very big proteins preferentially undergo secondary adsorption rather than primary adsorption via the heavily penalized compressive mechanism.

6. Are σ and N Independent?

In our discussion thus far, σ and N were considered as independent design parameters. In certain regimes this is indeed the case. In other situations the attained σ depends on N and on the binding energy of the anchor at the surface, ϵkT. If $\epsilon \gg 1$, the grafting density is largely determined by the surface density of grafting sites with the caveat that very high densities may prove unattainable for kinetic reasons. When ϵ is not too high, the maximal grafting density is set by the requirement that $F_{chain} \approx \epsilon kT$ or $\epsilon \approx N(a^2/\sigma)^{5/6}$.[22] This leads to

$$\sigma/a^2 \approx (N/\epsilon)^{6/5} \tag{32}$$

or $\xi_0/a \approx (N/\epsilon)^{3/5}$ and to

$$L_0/a \approx \epsilon^{2/5} N^{3/5} \tag{33}$$

In this case the performance of the brush of chains with a given N would improve as ϵ increases; that is, L_0 increases while σ decreases. However, increasing N for a certain ϵ will increase both σ and L_0, thus leading to a mixed effect on the anticipated performance of the layer.

7. Role of End Groups

Dense monolayers of oligo(ethylene glycol) alkanthiolates on gold are remarkably resistant to protein adsorption. In this case the number of ethylene glycol units involved can be as small as two.[23] However, in this system it appears that the controlling factor is the density and the configuration of the ethylene glycol end groups at the surface.[24,25] In such self-assembled monolayers the surface concentration of the end points is very high. This modifies the contact interaction between the protein and the surface. Osmotic interaction as discussed in the earlier sections plays no role in this situation. At the same time, it is unlikely that end groups play an important role in the interaction between proteins and polymer brushes. Their total surface density is $a^2/\sigma \ll 1$. In addition, the end points are not constrained to the exterior boundary, as is assumed in the Alexander model. Rather, they are distributed throughout the brush with a maximum at roughly $0.7L_0$. The configuration of the terminal segment in solution is also difficult to control. In the dense monolayers the self-assembly can be used to enforce a helical configuration. PEO chains in solutions and brushes of the chain apparently do contain helical domains, but their position along the chain trajectory is not determined and is likely to be random. It should be noted however that the chemical nature of the chain end groups may affect the chemical stability of the brush. Brushes formed from methyl-terminated PEO appear more stable than brushes formed from hydroxy-terminated chains.[26] This last observation has been rationalized in terms of preferential oxidation of the hydroxy-terminated PEO.

8. Concluding Remarks

Proteins are neither spheres nor cylinders. Flat monodispersed brushes are also an idealization. Modeling proteins as structureless colloidal particles clearly overlooks potentially important effects. One is the possibility of denaturation upon adsorption. This is likely to be a significant factor in the analysis of protein adsorption. It is however much less important in analyzing the repression of the adsorption. Another effect is expected for proteins, such as insulin, that exhibit a dynamic equilibrium involving unimers and a variety of multimers. Such equilibrium can affect the adsorption behavior onto a brush-coated surface. A unimer is more likely to undergo primary adsorption while multimers may be more susceptible to secondary adsorption. The analysis outlined above can be generalized to allow for such effects. With the reservations noted above, the simplifying assumptions listed are not likely to qualitatively modify the behavior of the system. In marked contrast, the choice of model adopted to describe the water soluble brush may give rise to qualitative effects. In this article, as in refs 7−9, the polymers are considered as "normal" flexible chains immersed in a simple fluid. It is thus possible to base the discussion on the comprehensive theoretical studies of brushes of normal polymers. This approximation is justified, with some important caveats, by experimental results. For example, it is consistent with the force profiles measured using the surface force apparatus (SFA) for both brushes,[27,28] and uniformly adsorbed layers[29,30] of PEO. It also provides a rationalization for a number of experimental results concerning the effects of brushes on protein adsorption. Nevertheless, the implementation of this "normal" polymer approximation requires caution. Water soluble polymers that form hydrogen bonds, and PEO in particular, exhibit distinctive traits having no counterpart among normal polymers. Three characteristics are of particular relevance: (i) Aqueous solutions of such polymers exhibit both upper and lower solution temperatures (UCST and LSCT, respectively).[31] On the other hand, the phase diagram of solutions of normal polymers in simple solvents, as described by the Flory theory and its refinements, involves only an UCST. (ii) Calorimetric data concerning aqueous solutions of PEO reveal a concentration dependent χ_{eff} when analyzed in terms of the Flory free energy.[32] In the case of normal polymers in

(22) Taunton, H. J.; Toprakcioglu, C.; Klein, J. *Macromolecules* **1990**, *23*, 571.
(23) Prime, K. L.; Whitesides, G. M. *J. Am. Chem. Soc.* **1993**, *115*, 1074.
(24) Deng, L.; Meksich, M.; Whitesides, G. M. *J. Am. Chem. Soc.* **1996**, *118*, 5136.
(25) Harder, P.; Grunze, M.; Dahint, R.; Whitesides, G. M.; Laibinis, P. E. *J. Phys. Chem. B* **1998**, *102*, 426.
(26) Harris, J. M. Conference on Non Fouling Surface Technologies, University of Washington, Seattle, WA, August 7−9, 1998.
(27) Claesson, P.; Kjellander, R.; Stenius, P.; Christensen, J. *J. Chem. Soc., Faraday Trans.* **1986**, *82*, 2735.
(28) Kuhl, T.; Leckband, D. E.; Lasic, D.; Israelachvili, J. N. *Biophys. J.* **1994**, *66*, 1479.
(29) Klein, J.; Luckham, P. *Adv. Colloid Interface Sci.* **1982**, *16*, 101; *Macromolecules* **1984**, *17*, 1041.
(30) Luckham, P.; Klein, J. *J. Chem. Soc., Faraday Trans.* **1990**, *86*, 2955.
(31) Goldstein, R. E. *J. Chem. Phys.* **1984**, *80*, 5340.

simple solvents, the Flory interaction parameter χ is constant. (iii) PEO chains can self-assemble into helices.[33,34] Normal polymers cannot form such secondary structures. A number of theoretical models were proposed to account for these features. These invoke different molecular mechanisms: interconversion of the PEO monomers between two isomeric states of different hydrophilicity,[35] solubilization of a hydrophobic backbone by labile hydrogen bonds,[36,37] and formation of clusters involving a number of monomers.[38] At this point the applicability of the different models has not been determined. However, the description of hydrogen-bonding hydrophilic polymers as normal polymers is clearly limited, and its range of applicability is yet to be established.

Recent experimental studies indeed suggest deviations from the normal polymer picture. Two examples illustrate this point. First, micelles formed by diblock copolymers incorporating a PEO block differ from those formed by normal diblock copolymers.[39] In particular, their aggregation number depends on the polymerization degrees of both blocks. The aggregation number of micelles of simple polymers is determined by the polymerization degree of the insoluble, core block alone. Second, SFA experiments involving compression of PEO brushes by a protein-coated surface are also difficult to rationalize within the normal polymer picture.[40] Two observations are of particular interest: (i) an onset of adhesion follows critical compression. (ii) The onset of adhesion is associated with a transition to a long-lived, dense, adhesive state of the brush. In principle, all of the three molecular models for PEO can rationalize this behavior. They suggest that a PEO brush may exhibit coexistence between two "phases": an inner, dense, hydrophobic phase and a dilute hydrophilic phase at the outer edge of the brush.[41,42] Within these models, the relative weight of the two phases is expected to vary with the grafting density and with compression, thus allowing for the deviations listed above.[43] In the context of our discussion, such coexistence may qualitatively modify U_{brush} by giving rise to an attractive inner region. At present it is not clear if these scenarios indeed occur. The possibility that the normal polymer approximation may not fully describe the interactions between proteins and polymer brushes requires study. The discussion of this problem in terms of the normal polymer picture is thus useful insofar as it leads to simple and testable predictions.

The normal polymer approximation suggests three guidelines for the design of polymer brushes that resist protein adsorption. First, large proteins may undergo secondary adsorption at the outer edge of the brush. "Cylindrical" proteins are especially likely to exhibit this behavior. This adsorption mode can be repressed by increasing the equilibrium thickness of the brush as $L_0 \sim R^{1/3}H^{2/3}$, where R is the radius of the cylinder and H is its height. Second, small globular proteins, $R < L_0$, are likely to adsorb at the surface itself. The thermodynamics and the kinetics of this primary adsorption mode depend primarily on the grafting density. This determines the osmotic penalty associated with the insertion of the protein into the brush. The corresponding activation barrier is $U^*/kT \approx (R/\sigma^{1/2})^3$, where the associated rate constant is $k_{\mathrm{ads}} \sim \exp(-U^*/kT)$. A significant effect on the adsorption isotherm is similarly expected when the osmotic penalty is large compared to $|U_{\mathrm{ads}}|$. This suggests that, for a protein of radius R, the minimal grafting density to repress adsorption is specified by $\sigma_{\mathrm{co}} \approx R^2(kT/|U_{\mathrm{ads}}|)$. Finally, it is important to note that the grafting density can depend on N in such cases and that σ and L_0 are not independent design parameters.

9. Appendix I: The Kramers Rate Theory

The local chemical potential of a particle experiencing an external potential $U(z)$ is

$$\mu(z) = U(z) + kT \ln c(z) \tag{34}$$

where $c(z)$ is the local concentration. Spatial variation of $\mu(z)$ induces a flux, $j = cv_{\mathrm{f}}$, leading to a uniform and constant $\mu(z)$. The average velocity of this flux v_{f} is

$$v_{\mathrm{f}}\zeta = -\frac{\partial \mu}{\partial z} \tag{35}$$

where ζ is a friction coefficient related to the diffusion coefficient D as $D = kT/\zeta$. Note that this local relationship also applies when ζ is position dependent. For spherical particles ζ is given by the Stokes equation

$$\zeta = 6\pi\eta R \tag{36}$$

The corresponding flux is thus[44]

$$j = -\frac{c}{\zeta}\frac{\partial \mu}{\partial z} \tag{37}$$

The resulting expression, a generalization of Fick's law

$$j = -D\frac{\partial c}{\partial z} + \frac{Dc}{kT}\frac{\partial U}{\partial z} = D\exp(-U/kT)\frac{\partial}{\partial z}c\exp(U/kT) \tag{38}$$

is the starting point for the high-viscosity limit of the Kramers rate theory.[14] It involves a steady-state solution, $j =$ constant, representing, in our case, a stationary one-dimensional flux from the bulk phase to the adsorbing surface. The concentration profile and energy distribution at the boundary of the brush are assumed to equilibrate rapidly in comparison to the adsorption process. As a result, the concentration and energy distribution at the edge of the brush correspond to the bulk situation. Interactions between the particles are ignored. The analysis focuses on the initial state when no particles populate the inner free energy well located at the adsorbing surface. With this in mind, we integrate the constant j as given by the right hand side of eq 38, between z_{in}, the position of the inner minimum, and z_{bulk}, the outer boundary of the brush. z_{bulk} is defined as the minimal z for which $U_{\mathrm{brush}}(z_{\mathrm{bulk}}) = 0$, that is, $z_{\mathrm{bulk}} \approx L_0$. This leads to

(32) Molyneux, P. In *Water*; Franks, F., Ed.; Plenum: New York, 1975; Vol. 4.
(33) Tadokoro, Y.; Chatini, Y.; Yoshihara, T.; Thara, S.; Murahashi, S. *Makromol. Chem.* **1964**, *73*, 109.
(34) Koenig, J. L.; Angwood, A. C. *J. Polym. Sci., Polym. Phys. Ed.* **1970**, *8*, 1787.
(35) Karlstrom, G. *J. Phys. Chem.* **1985**, *89*, 4962.
(36) Matsuyama, A.; Tanaka, F. *Phys. Rev. Lett.* **1990**, *65*, 341.
(37) Bekiranov, S.; Bruinsma, R.; Pincus, P. *Europhys. Lett.* **1993**, *24*, 183; *Phys. Rev. E* **1997**, *55*, 577.
(38) de Gennes, P. G. *C. R. Acad. Sci., Ser. II* **1991**, *313*, 1117.
(39) Jada, A.; Hurtrez, G.; Siffert, B.; Riess, G. *Macromol. Chem. Phys.* **1996**, *197*, 3697.
(40) Sheth, S. R.; Leckband, D. *Proc. Natl. Acad. Sci. U.S.A.* **1997**, *94*, 8399.
(41) Bjorling, B.; Linse, P.; Karlstrom, G. *J. Phys. Chem.* **1990**, *94*, 471.
(42) Wagner, M.; Brochard-Wyart, F.; Hervet, H.; de Gennes, P. G. *Colloid Polym. Sci.* **1993**, *271*, 621.
(43) Halperin, A. *Eur. Phys. J.* **1998**, *3*, 359.
(44) Doi, M.; Edwards, S. F. *The Theory of Polymer Dynamics*; Oxford University Press: Oxford, U.K., 1986.

$$j = \frac{Dc\,\exp(U/kT)\big|_{z_{bulk}}^{z_{min}}}{\int_{z_{bulk}}^{z_{min}} \exp(U/kT)\,dz} \tag{39}$$

With our choice of the bulk as a reference state and since $c(z_{min}) = 0$ and $c(z_{bulk}) = c$, the numerator is $Dc\exp(U/kT)$. The denominator is evaluated, approximately, by expanding $U(z)$ around it maximum at z^* in powers of $(z - z^*)$. Retaining terms up to second order, $U \approx U^* - (w/2)(z - z^*)^2$. The denominator becomes $\exp(U^*/kT)\int_{z_{bulk}}^{z_{min}} \exp[-w(z - z^*)^2\,dz$. Since this integral is dominated by the contribution from $z \approx z^*$, we may change the integration limits to $\pm\infty$, thus leading to $(2\pi kT/w)^{1/2}$. In turn, the width of the barrier kT below U^*, α, is $kT/w \approx \alpha^2$.[15] Altogether the steady-state flux is

$$j \approx -\frac{Dc\,\exp(-U^*/kT)}{\alpha} \tag{40}$$

The characteristic time to diffuse across the barrier $\tau_{barrier}$ is specified by Einstein's diffusion relation $D\tau_{barrier} \approx \alpha^2$. Accordingly, $D/\alpha \approx \alpha/\tau_{barrier} \approx v_{barrier}$ is the flux velocity across the barrier. j may be thus expressed as $j = cv_{diff}$, where $v_{diff} \approx \exp(-U^*/kT)v_{barrier}$. The characteristic time for crossing a barrier of overall thickness L_0 is accordingly v_{diff}/L_0, leading to the rate constant presented in section 2.

10. Appendix II: Viscosity in Semidilute Solutions

The viscosity experienced by an object moving through a semidilute solution of entangled polymers is expected to depend on the size of the object R.[20] To quantify this expectation, we first recall the essential features of the macroscopic viscosity and then formulate a scaling argument for the R dependence of $\eta(R)$. The macroscopic viscosity of a semidilute solution of entangled polymers is $\eta \approx E\tau_{rep}$. Here, E is the elastic modulus of the transient network $E \approx kT/\xi^3$. τ_{rep} is the reptation time of the chain when viewed as a string of N/g blobs of size $\xi \approx g^{3/5}a$. τ_{rep} is the time required for the chain to diffuse along its own trajectory. The length of the trajectory is $L_t \approx (N/g)\xi$. The diffusion coefficient of a chain undergoing reptation is $D_{rep} \approx kT/\eta_s L_t$, where η_s is the viscosity of the pure solvent. The Einstein diffusion relation yields $\tau_{rep} \approx L_t^2/D_{rep} \approx \eta_s L_t^3/kT \approx (N/g)^3\tau_{blob}$. τ_{blob} is the Zimm time of the blob, that is, the time required for the blob to diffuse its own length. The diffusion constant for the blob is $D_{blob} \approx kT/\eta_s\xi$, and the Einstein relation leads to $\tau_{blob} \approx \xi^2/D_{blob} \approx \eta_s\xi^3/kT$. Altogether

$$\eta \approx \eta_s(L_t/\xi)^3 \approx \eta_s(N/g)^3 \tag{41}$$

This is the viscosity encountered by a macroscopic object, $R \gg \xi$, moving through the solution. A very small object, $R \lesssim \xi$, is however expected to experience the viscosity of the pure solvent η_s. The viscosity experienced by objects of intermediate size depends on R. Large objects, $R > L_t$, perturb whole chains, thus giving rise to $\eta \sim t_{rep}$. Smaller objects are expected to perturb only part of the chain, thus leading to smaller characteristic times. This suggests that $\eta(R)$ should be a function of R/L_t. One may argue that $\eta(R) \approx \eta\Phi(R/L_t)$, where $\Phi(R/L_t)$ is a scaling function such that $\Phi(R/L_t) \approx 1$ when $R \approx L_t$ and $\Phi(R/L_t) \approx (R/L_t)^x$ when $R \ll L_t$. Since $\eta(R)$ for $R \ll L_t$ should not depend on L_t, we find $x = 3$ or

$$\eta(R) \approx \eta_s(R/\xi)^3 \qquad \xi < R < L_t \tag{42}$$

This leads, as desired, to $\eta(R) \approx \eta_s$ for $R \leq \xi$ and to $\eta \approx \eta_s(L_t/\xi)^3$ for $R \geq L_t$. As noted, this discussion concerns solution of entangled polymers. However, grafted chains in a flat brush are highly stretched in equilibrium. Consequently, they exhibit reptative dynamics even in the absence of entanglements.

Acknowledgment. This work benefited from instructive discussions with D. Leckband, M. Malmsten, T. Kuhl, and P. Pincus. It was supported in part by a NATO Collaborative Research Grant, CRG 950845, and by a CNRS-NSF, U.S.−France Cooperative Research, Grant.

LA981356F